Earthquake Geotechnical Engineering for Protection and Development of Environment and Constructions – Silvestri & Moraci (Eds)
© 2019 Associazione Geotecnica Italiana, Rome, Italy, ISBN 978-0-367-14328-2

Influence of earthquake-induced pore-water pressure on the seismic stability of cohesive slopes

G. Di Filippo, G. Biondi & E. Cascone
University of Messina, Italy

ABSTRACT: In the seismic stability analysis of natural slopes the possibly occurring weakening effects due to excess pore-water pressures and cyclic degradation are generally neglected or not properly accounted for. Accordingly, the evaluation of the seismic performance of a slope may result unreliable. The paper describes a simplified procedure for the evaluation of the seismic stability conditions of clay slopes taking into account the possible occurrence of cyclic strength degradation due to excess pore water pressures. An experimental-based model was adopted to predict the occurrence and the magnitude of the excess pore-water pressure, starting from an assessment of the earthquake-induced shear strain level. The results of the numerical analyses presented in the paper show that the amplitude of the horizontal acceleration and the plasticity of the soil are the main responsible of the occurrence of weakening and inertial-weakening instabilities.

1 INTRODUCTION

Seismic induced landslides represent one of the most damaging collateral hazards associated with large earthquakes. Post earthquake reports have given evidence of the severe social and economical consequences of these phenomena. Frequently, the damages induced by earthquake-triggered landslides exceed those directly related to the ground shaking and were frequently ascribed to the effects of cyclic behaviour of soils (Nakamura et al. 2014). In fact, during strong earthquakes soils develop significant deformations that may affect the stability conditions of natural slopes possibly causing failure and involving significant losses in terms of damages to environment, structures and lifelines (Harp and Jibson, 1990; Biondi et al. 2004). Furthermore, evidence of past earthquakes showed also that topographic irregularities significantly affect seismic site response and, in many cases, are responsible of large amplifications of the ground motion and of severe damages to structures and lifelines.

The effects of the cyclic reduction of soil shear strength are frequently disregarded in the procedures aimed to the evaluation of the seismic stability conditions and to the assessment of the post-seismic serviceability of the structures and of the infrastructures which may interact with the slope. In fact, rigorous 2D and 3D dynamic non-linear analyses should be applied involving a suitable selection of the input ground motion and an advanced constitutive modeling based on a proper geotechnical characterization. As a consequence, simplified estimates are frequently performed neglecting most of the effects related to the cyclic behaviour of soils. In these cases, if the analysis neglects the strength and stiffness reduction due to the excess pore-water pressure, it could lead to an unsafe estimation of the slope seismic response.

Seismic performance of slopes can be evaluated through different methods of analysis requiring different level of accuracy for appropriate problem formulation, modeling of mechanical soil behaviour and analysis procedures. In this framework, the displacement-based approach represents a good compromise between computational effort and results accuracy and has the advantage of providing a quantitative assessment of earthquake-induced displacement using a rather simple numerical procedure. In the original of Newmark's sliding block analysis, the effects of possible reduction of soil shear strength (and in turn of critical

acceleration) and of the change in slope geometry during the motion (Bandini et al. 2015, Ingegneri et al. 2019), are not taken into account. A procedure to assess the influence of earthquake-induced pore-water pressure on the behaviour of slopes is presented in the paper. An experimental-based pore-water pressure generation model was adopted to perform an effective stress analysis with reference to the infinite slope scheme accounting for the reduction of the critical acceleration due to the strength reduction. The numerical results show that the occurrence of weakening and inertial-weakening instabilities strongly depend on the amplitude of the horizontal acceleration and on the plasticity of the soil.

2 REFERENCE SLOPE SCHEME

To analyze the effects of the possible reduction in soil shear strength the infinite slope scheme (Figure 1), which provides the most conservative value of the critical acceleration, was considered. This scheme is suitable for slopes characterized by translational failure mechanism, with shallow and wide sliding surface. The stability conditions are evaluated with the limit equilibrium method, using the pseudo-static approach, assuming a rigid-plastic behaviour of the unstable soil and a uniform reduction of the soil shear strength along the sliding surface.

The slope stability condition is described by the static safety factor F_s (eq. 1), the seismic safety factor F_d (eq. 2) and the horizontal component of the critical seismic coefficient $k_{H,c}$ (eq. 3)

$$F_s = \frac{c'/(\gamma \cdot D)}{\sin\beta} - + \frac{\tan\phi'}{\tan\beta} \cdot (1 - r_u) \tag{1}$$

$$F_d = \frac{c'/(\gamma \cdot D) + [\cos\beta \cdot (1 - r_u) \cdot (1 - \Delta u^*) - k_H \cdot (\sin\beta \pm \Omega \cdot \cos\beta)] \cdot \tan\varphi'}{\mathrm{sen}\beta + k_H \cdot (\cos\beta \mp \Omega \cdot \sin\beta)} \tag{2}$$

$$k_{H,c} = \frac{c'/(\gamma \cdot D) + \cos\beta \cdot \tan\varphi' \cdot (1 - r_u) \cdot (1 - \Delta u^*) - \mathrm{sen}\beta}{(\cos\beta \mp \Omega \cdot \sin\beta) + \tan\varphi' \cdot (\sin\beta \pm \Omega \cdot \cos\beta)} \tag{3}$$

In equations (1), (2) and (3), γ is the soil unit weight, c' and φ' are the effective cohesion and the angle of shearing resistance along the sliding surface, respectively; β is the slope angle; D is

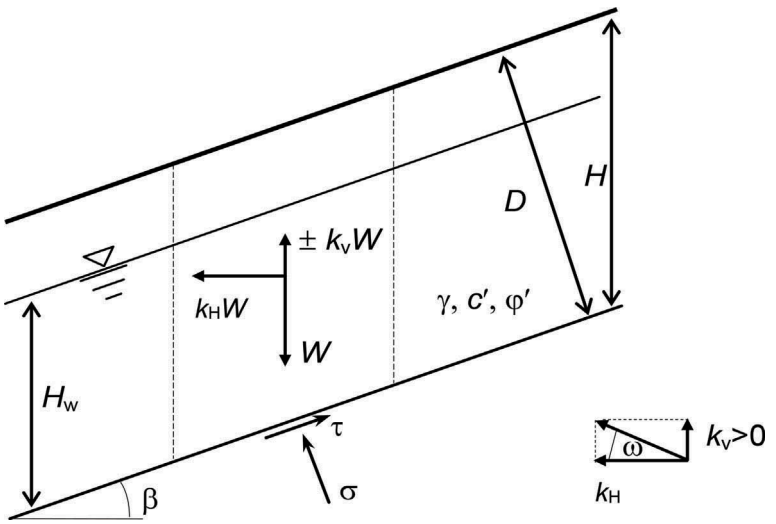

Figure 1. Reference slope scheme and relevant notations

the thickness of the sliding mass; $r_u = u_0/\sigma_0$ is the static pore water pressure coefficient defined as the ratio between the pore water pressure (u_0) and static total stress (σ_0) acting normally to the potential sliding surface; $\Delta u^* = \Delta u/\sigma'_0$ is the earthquake induced pore pressure ratio defined as the ratio between the earthquake induced pore pressure (Δu) and the static effective stress (σ'_0) acting normally to the potential sliding surface; $\Omega = \tan \omega = k_v/k_h$ is the ratio between the vertical (k_v) and horizontal (k_H) component of the seismic acceleration coefficient ($\Omega>0$ for k_v directed upwards). In equation (2) k_H and Δu^* represent, respectively, the inertial and weakening effects on the slope stability conditions. The presence of the term Δu^* in eq. (3) implies a reduction of the critical acceleration coefficient over the time, starting from its initial value $k_{H,co}$ (eq. 4) down to a minimum value $k_{H,cmin}$ (eq. 5), which is attained when the earthquake induced pore pressure ratio (Δu^*) attains its maximum value (Δu^*_{max}).

$$k_{H,co} = \frac{c'/(\gamma \cdot D) + \cos\beta \cdot \tan\phi' \cdot (1 - r_u) - \text{sen}\beta}{(\cos\beta \mp \Omega \cdot \sin\beta) + \tan\phi' \cdot (\sin\beta \pm \Omega \cdot \cos\beta)} \tag{4}$$

$$k_{H,cmin} = \frac{c'/(\gamma \cdot D) + \cos\beta \cdot \tan\phi' \cdot (1 - r_u) \cdot (1 - \Delta u^*_{max}) - \text{sen}\beta}{(\cos\beta \mp \Omega \cdot \sin\beta) + \tan\phi' \cdot (\sin\beta \pm \Omega \cdot \cos\beta)} \tag{5}$$

3 PROPOSED PROCEDURE

Starting from the results of undrained cyclic triaxial tests, Matsui et al. (1980) developed a model for the prediction of the residual pore-water pressure for both *NC* and *OC* clays subjected to uniform cyclic loading. The residual pore-water pressure is expressed in terms of excess pore-water pressure ratio Δu^* which depends on the maximum shear strain $\gamma_{c,max}$ and on the volumetric threshold value of the shear strain γ_v (eq. 6).

$$\Delta u^* = \frac{\Delta u}{\sigma' c} = 0.45 \cdot \log \frac{\gamma_{c,max}}{\gamma_v} \tag{6}$$

The use of such kind of predictive model in the case of irregular loading history generally requires the conversion of the earthquake-induced irregular loading history into an equivalent uniform one (Biondi et al. 2012). Accordingly the maximum shear strain $\gamma_{c,max}$ was assumed herein equal to an average shear strain level γ_{ave} compatible to an average value τ_{ave} of the shear stress time-history imposed by the earthquake.

Accordingly, the procedure adopted for the assessment of Δu^* consists of the following steps:

- estimation of an average amplitude τ_{ave} of the shear stress time-history induced by the earthquake at the depth of the potential sliding surface
- evaluation of the compatible shear strain level γ_{ave} introducing a proper constitutive model
- evaluation of the volumetric threshold value γ_v of the shear strain level
- computation of the excess pore-water pressure ratio through eq. (6) if $\gamma_{ave} > \gamma_{v.}$

3.1 *Evaluation of the shear strain level* γ_{ave}

Denoting with $G(\gamma)$ and G_o, the shear modulus for a given shear strain level γ and the small strain shear modulus, respectively, γ_{ave} can be computed through eq. (7):

$$\gamma_{ave} = \frac{\tau_{ave}}{G(\gamma_{ave})} = \frac{0,65 \cdot \gamma \cdot D \cdot k_H(\cos\beta \pm \Omega \cdot \sin\beta) \cdot r_d/G_o}{G(\gamma_{ave})/G_o} \tag{7}$$

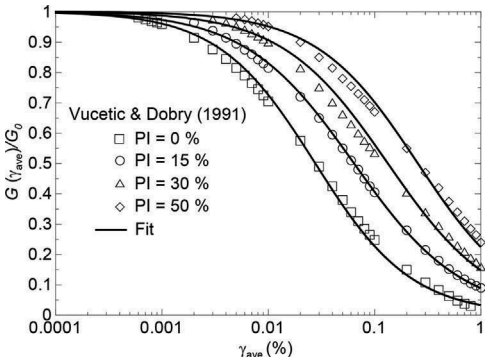

Figure 2. Shear modulus reduction curves adopted in the analyses

Table 2. Values of the fitting constants adopted to describe the normalized shear modulus reduction curves.

PI (%)	*a*	*b*
0	30,546	0,955
15	10,385	0,853
30	5,799	0,874
50	3,468	0,913

In the previous equation τ_{ave} denote an average shear stress amplitude estimated introducing the effect of the soil compliance through the stress reduction factor $r_d = 1–0.015H$ (Iwasaki et al. 1978), and considering the transient nature of the earthquake-induced shear stress time-history by means of an equivalent stress level α equal to 0.65; $G(\gamma_{ave})/G_o$ denotes the shape of the shear modulus reduction curve. For cohesive soils this shape is influenced by the plastic index *PI* and the effective confining pressure. Accordingly, the curves proposed by Vucetic and Dobry (1991) (Figure 2) for $PI=0\div50\%$ were adopted herein.

Using eq. (7), γ_{ave} can be iteratively computed. To this purpose the curves proposed by Vucetic and Dobry (1991) were fitted using the relationship described in table 2 together with the two fitting constants *a* and *b*. The expression by D'Onofrio and Silvestri (2001) for *NC* clays was adopted to compute the dependence of G_o on the effective confining pressure and *PI*.

$$G(\gamma_{ave})/G_o = 1/\left(1 + a \cdot \gamma_{ave}^{b}\right) \tag{8}$$

Using this procedure, for a given slope scheme (i.e for given values of γ, *D*, r_u, β, φ', *PI*) and design earthquake (i.e for given values of k_H and Ω), γ_{ave} can be computed. As an example, for the case $\gamma = 20$ kN/m^3, $D = 10$ m, $r_u = 0.5$, φ' = 25° and Ω = 0, Figure 3a describes the computed average strain level for k_H ranging from 0 to 0.3 and several values of *PI*. From the data it is evident a nonlinear relationship between k_H and γ_{ave} and a significant influence of both *PI* and k_H on the computed values; the obtained k_H-γ_{ave} nonlinear relationship must be

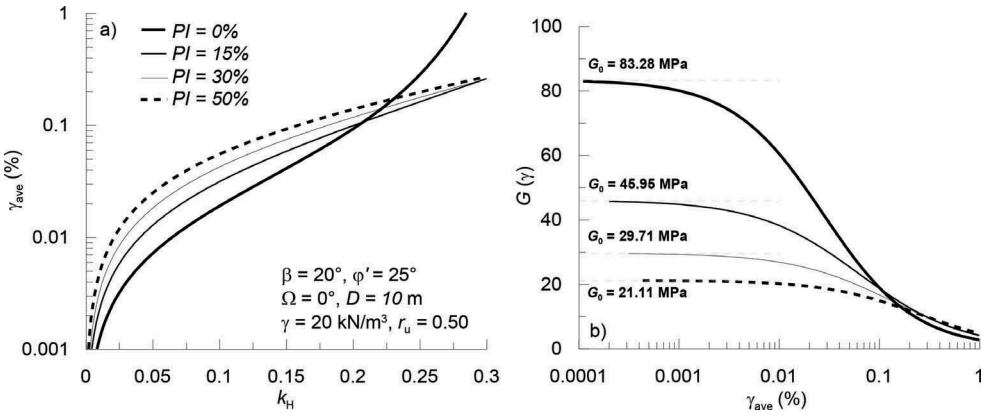

Figure 3. Influence of the Plasticity Index *PI* (%) on the shear strain (a) and the shear modulus decay (b).

ascribed to the adopted constitutive model that assumes a non-linear decay of the shear modulus (Figure 3b).

3.2 *Evaluation of the threshold value* γ_v

As a result the analysis of a large number of experimental data related to cohesive soils, Vucetic and Dobry (1991) investigated the effects of the plasticity index on the volumetric threshold shear strain and provided upper and lower limits (continuous grey lines in Figure 4a,b) together with the average curve depicted as a dashed grey line in Figure 4a and b.

More recently Hsu and Vucetic (2002, 2006) and Mortezaie and Vucetic (2016) showed that, for *NC* clays, the values of γ_v are close to the lower limit proposed by Vucetic and Dobry (1991); according to Mortezaie and Vucetic (2016) γ_{td} is the amplitude below which there is practically no cyclic degradation and γ_{tp} is the amplitude below which there is practically no permanent cyclic pore water pressure change with the cyclic number N.

The values of γ_v provided by Matsui et al. (1980) are also represented in Figure 4b and range between the average curve and the upper limit proposed by Vucetic and Dobry (1991). Herein the lower limit proposed by Vucetic and Dobry (1991) will be used as reference for the evaluation of the volumetric threshold for *NC* clays.

For different values of the plasticity index, it is possible to define threshold values $k_{H,v}$ of the horizontal seismic coefficient below which the earthquake-induced shear strain level do not produce excess pore water pressure. Through a combined use of eq. (7) and (8), and imposing $\gamma_{ave} = \gamma_v$ the following expression can be obtained:

$$k_{H,v} = \frac{G_o}{0,65 \cdot \gamma \cdot H \cdot (\cos\beta \pm \Omega \cdot \sin\beta) \cdot \cos\beta \cdot r_d} \cdot \frac{\gamma_v}{1 + a \cdot \gamma_v^b} \tag{9}$$

Figure 5 illustrates the threshold values $k_{H,v}$ for different values of *PI,* r_u and of the thickness D of the sliding soil mass. From the data plotted in Figure 5 it is apparent that the condition $k_H > 0.15$ introduced by Eurocode 8 (2003) to detect the possibly occurrence of strength degradation and increase in pore pressure in saturated soils may lead to unsafe estimate for $PI < 30\%$. Specifically, strength reduction due to excess of pore water pressure may also occur at acceleration levels lower than 0.15g depending on the static effective stress state acting along the potential sliding surface reflected in the value of r_u.

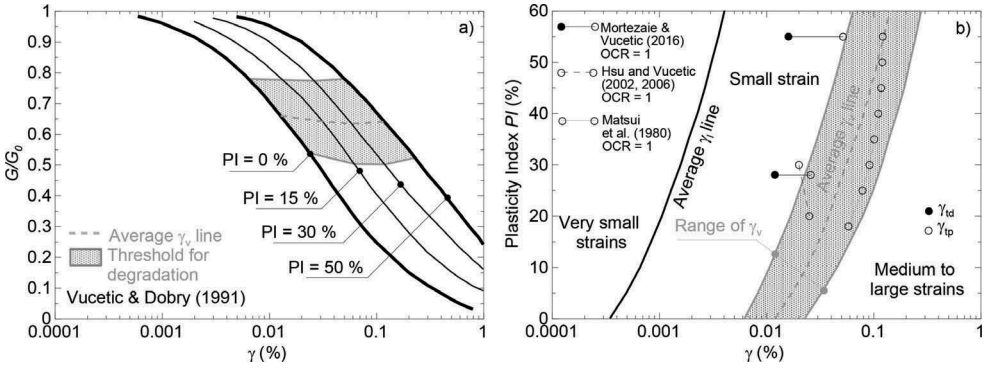

Figure 4. Threshold strains for degradation of clay with different plasticity index: data from Vucetic and Dobry (1991) (a) and comparison with literature data (b).

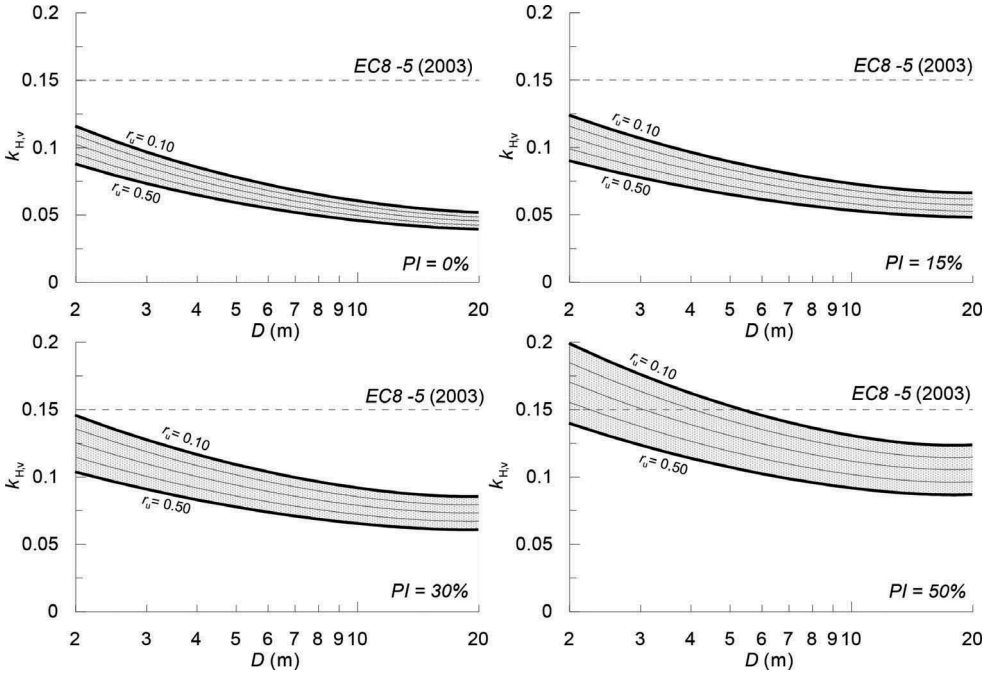

Figure 5. Threshold values of the horizontal seismic coefficient (β=20°, φ'=25°, γ =20 kN/m^3, Ω=0).

3.3 *Excess pore-water pressure ratio*

Starting from the computed values of γ_{ave}, the condition $\gamma_{ave} > \gamma_v$ can be checked and, if required, the excess pore-water pressure ratio Δu^* can be computed using eq. (6). The values of Δu^* evaluated with the proposed procedure are plotted in Figure 6 for the same combination of the slope and earthquake parameters considered in Figure 3. In Figure 3 a significant influence of both *PI* and k_H on Δu^* is apparent. In order to detect the parameters more influent on the computed Δu^*, a parametric analysis was carried out. The slope angle β and the angle of shear strength φ' slightly affect the values of Δu^* while the more relevant influence of the static pore pressure ratio r_u and of the thickness of the layer *D* on the computed values of Δu^* is shown in Figure 7 for the case *PI*=15%, φ'=25° and Ω=0. The influence of the vertical component of the seismic acceleration is not investigated in this paper (Ω=0).

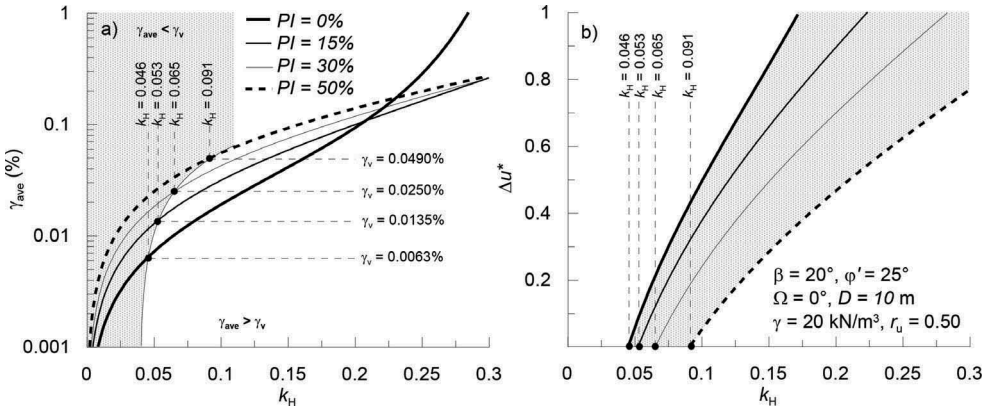

Figure 6. Evaluation of the threshold values of γ_v (a) and k_H (b) for different values of *PI*.

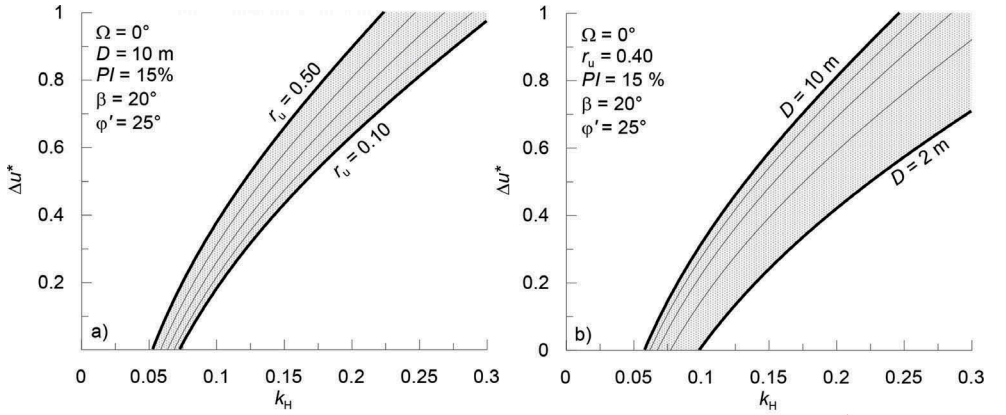

Figure 7. – Influence of r_u and D on the excess pore water pressure ratio Δu^*.

3.4 *Threshold values of the excess pore water pressure ratio*

Two threshold values, Δu_f^* and Δu_d^*, of Δu^* were introduced herein allowing to detect the causes of the possibly occurring instability and the proper approach for the slope displacements analysis. To define the threshold values, the expressions of the effective stress state acting in both static and seismic conditions, the expressions of the static F_s (eq. 1) and pseudo-static F_d (eq. 2) safety factor, and finally the expressions giving the initial $k_{H,co}$ (eq. 4) and the current value $k_{H,c}$ (eq. 3) of the slope critical acceleration are required.

Δu_f^* represents the earthquake induced pore-water pressure ratio that makes the available shear strength mobilized along the potential sliding surface equal to the minimum static shear stress required to maintain equilibrium; therefore, the condition $\Delta u^* = \Delta u_f^*$ leads to a null value of the critical acceleration coefficient (eq. 4).

Δu_d^* is the value of Δu^* beyond which the reduction of soil shear strength is high enough to bring the initial slope critical acceleration $k_{H,co}$ below peak value $k_{H,max}$ of the earthquake acceleration. Hence, in the framework of a Newmark-type analysis, if the condition $\Delta u^* = \Delta u_d^*$ is attained, permanent displacements may occur in the slope even if it was seismically stable (i.e. $k_{H,co} \geq k_H$) before the occurrence of the strength reduction; therefore $\Delta u^* = \Delta u_d^*$ makes the pseudo-static safety factor F_d equal to unity (eq. 2). Imposing $k_{H,cmin} = 0$ and F_d=1 the following values of Δu_f^* (eq. 10) and Δu_d^* (eq. 11) were derived:

$$\Delta u_f^* = (F_s - 1) \cdot \tan\beta / [\tan\phi' \cdot (1 - r_u)] \tag{10}$$

$$\Delta u_d^* = \Delta u_f^* \cdot \left(1 - k_H / k_{H,co}\right) \tag{11}$$

To describe the influence of the excess pore-water pressure on the displacement response of the slope, the reduction in the critical acceleration due to the strength reduction must be considered. To this purpose two values $k_{H,co}$ eq. (4) and $k_{H,cmin}$ eq. (5) of the slope critical acceleration can be computed: $k_{H,co}$ refers to the initial condition, before the excess pore-water pressure takes place, and represents the value of the slope critical acceleration to be adopted in a displacement analysis which neglects the effect of the strength reduction. Otherwise $k_{H,cmin}$ represents the value to which the slope critical acceleration reduces when the maximum value of the excess pore-water pressure is attained. If no excess-pore-water pressure develops in the soil ($\gamma < \gamma_v$ and Δu^*=0), $k_{H,c}$ equals $k_{H,co}$; otherwise ($\gamma > \gamma_v$ and $\Delta u^* > 0$), the reduction of $k_{H,c}$ from $k_{H,co}$ to $k_{H,cmin}$ must be considered in the displacements analysis.

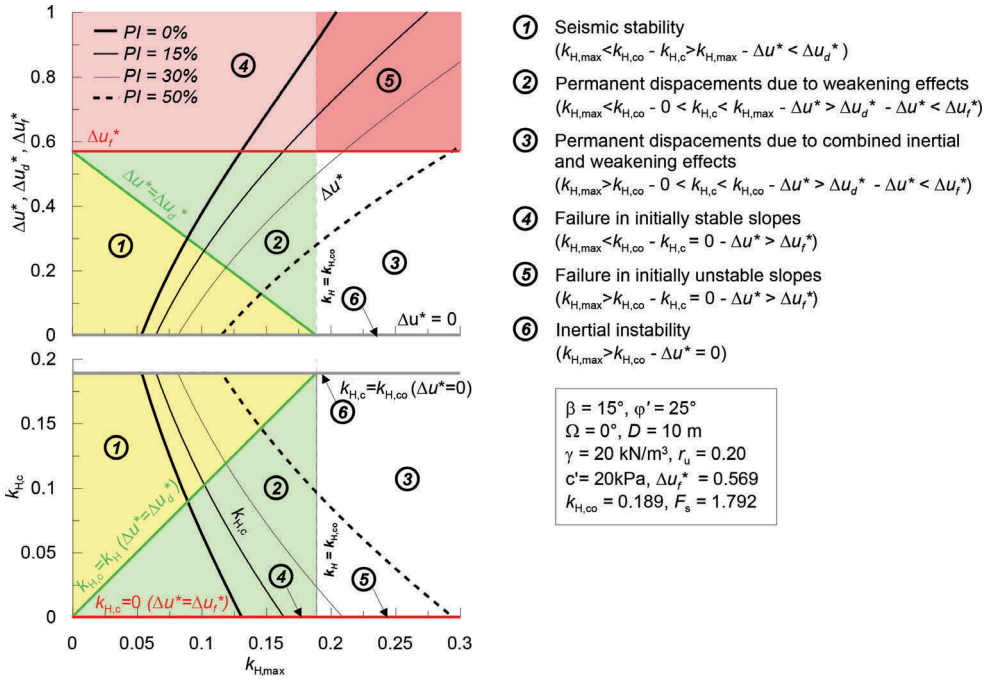

Figure 8. Stability charts in terms of (a) excess pore pressure ratio (b) critical acceleration coefficient.

4 DISPLACEMENT EVALUATION AND PROPOSED STABILITY CHARTS

In order to describe the application of the proposed procedure, a slope scheme with γ=20kN/m^3, D=10m, φ'=25°, r_u=0.20, β=15° and $c'/(\gamma D)$ = 0.10 was considered; from eq. (4) and eq. (10), it is $k_{H,co}$=0.189 and Δu_f^*=0.569. The comparison between Δu^* and the threshold values Δu_f^* and Δu_d^* is shown in Figure 8a for different values of PI; the same comparison in terms of critical acceleration coefficient is shown in Figure 8b. The plots of Figure 8 can be considered as an example of the stability charts.

The zone 1 in Figure 8 represents slopes characterized by $\Delta u_d^*>0$, $k_H/k_{H,co}<1$, for which the stability conditions are maintained during the earthquake despite the strength reduction ($\Delta u^*<\Delta u_d^*$, $k_H<k_{H,cmin}$) or in the case of no strength reduction ($\Delta u^*=0$ if $\gamma<\gamma_v$ and $k_H<k_{H,v}$). In the same figure the zones 2 and 3 represent slopes for which permanent displacements during the earthquake may occur. Specifically, points in zone 2 represent slopes characterized by initial conditions of seismic stability ($\Delta u_d^*>0$, $k_H/k_{H,co}<1$), in which permanent displacements develop even if a failure condition is not attained ($\Delta u_d^*<\Delta u^*<\Delta u_f^*$, $k_H>k_{H,cmin}$).

The points that fall in zone 3 represent slopes ($k_H/k_{H,co}>1$), in which displacements are due to both the inertial and the weakening effects. In this case, if no significant change in shear strength occurs ($\Delta u^*=0$, $k_{H,co}=k_{H,cmin}$), the displacement analysis can be carried out using the original Newmark sliding block method and the initial value of the critical seismic coefficient $k_{H,co}$ (inertial instability, zone 6); conversely, if the permanent displacements are due to inertial and weakening effects a modified Newmark-type analysis accounting for the strength reduction must be used. Finally, for points falling into zones 4 and 5 ($\Delta u^*>\Delta u_f^*$, $k_{H,cmin}=0$) the earthquake induced pore pressure leads to the collapse. Depending on the threshold value Δu_d^*, the mechanism may occur in slopes initially stable (zone 4, $\Delta u_d^*>0$) or unstable (zone 5, $\Delta u_d^*=0$) under seismic conditions. In the first case, the collapse can only be predicted if the possible reduction in shear strength is taken into account in the analysis.

ACKNOWLEDGEMENT

This work is a part of the research activities carried out by the Messina Research Unit in the framework of the work package WP2-Slope Stability of a Research Project funded by the ReLuis (University Network of Seismic Engineering Laboratories) consortium (Attuazione Progetto Esecutivo Convenzione DPC/ReLUIS 2018 – AQ DPC/ReLUIS 2014-2018).

REFERENCES

Bandini V., Biondi G., Cascone E., Rampello S. 2015. A GLE-based model for seismic displacement analysis of scope including strength degradation and geometry rearrangement. *Soil Dynamics and Earthquake Engineering*, *(*71): pp. 128–142.

Biondi G., Cascone E., Di Filippo G. 2012. Affidabilità di alcune correlazioni empiriche per la stima del numero di cicli di carico equivalente. *Rivista Italiana di Geotecnica* 2012; XLVI (2): 9–39.

Biondi G., Condorelli A., Maugeri M., Mussumeci G. 2004. Earthquake-triggered landslide hazards in the Catania area. *WIT Transactions on Ecology and the Environment*, 77.

D'Onofrio A., Silvestri F. 2001. Influence of micro-structure on small-strain stiffness and damping of fine drained soils and effects on local site response. *IV Int. Conf. on 'Recent Advances in Geotechnical Earthquake* Engineering *and* Soil Dynamics'. S. Diego, CA, paper 1.19.

Eurocode 8-5, 2003. EN 1998-1 (2003). Eurocode 8: Design of structures for earthquake resistance - Part 5: Foundations, retaining structures and geotechnical aspects. *CEN European Committee for Standardization*, Brussels, Belgium.

Harp E.L., Jibson R.W. 1996. Landslides triggered by the 1994 Northridge, California, earthquake. *Bulletin of the Seismological Society of America*, 86(1B), S319–S332.

Hsu C.C.,Vucetic M. 2002. Dynamic and cyclic behaviour of soils over the wide range of shear strains in NGI-type simple shear testing device. *Research Rep. No. UCLA ENG-02-228*, Civil and Environmental Engineering Dept., Univ. of California, Los Angeles.

Hsu C.C., Vucetic M. 2006. Threshold Shear Strain for Cyclic Pore-Water Pressure in Cohesive Soils. *J. Geotech. Geoenviron. Eng*. 2006.132:1325–1335.

Ingegneri S., Di Filippo G., Biondi G., Cascone E. 2019. Influence of cyclic strength degradation on the results of a newmark-type analysis. This Conference.

Iwasaki T., Tatsuoka F., Tokida K., Yasuda S. 1978. A practical method for assessing soil liquefaction potential based on case studies at various sites in Japan. *II Int. Conf. on Microzonation*.

Matsui T., Ito T., Ohara H, 1980. Cyclic stress-strain history and shear characteristics of clay. *Journal of Geotechnical Engineering*, ASCE, 106 (10),1101–1120, 1980.

Mortezaie A., Vucetic M. 2016. Threshold Shear Strains for Cyclic Degradation and Cyclic Pore Water Pressure Generation in Two Clays. *J. Geotech. Geoenviron. Eng*., 2016, 142 (5).

Nakamura S., Wakai A., Umemura J., Sugimoto H., Takeshi T. 2014. Earthquake-induced landslides: Distribution, motion and mechanisms. *Soils and Foundations*. Vol. 54, Issue 4, pp. 544–559.

Vucetic M., Dobry R. 1991. Effects of the soil plasticity on cyclic response. *Journal Geoth. Eng. Division*, ASCE, 120, No. 12.